ANS PROCEEDINGS

1985 NATIONAL HEAT TRANSFER CONFERENCE

August 4-7, 1985
Denver, Colorado

Published by the American Nuclear Society

SPONSORED BY THE THERMAL HYDRAULICS DIVISION OF THE AMERICAN NUCLEAR SOCIETY

PROCEEDINGS

ANS PROCEEDINGS

1985 NATIONAL HEAT TRANSFER CONFERENCE

Technical Sessions

Sponsored by

THERMAL HYDRAULICS DIVISION

AMERICAN NUCLEAR SOCIETY

AUGUST 4 - AUGUST 7, 1985

DENVER, COLORADO

Printed in USA

ISBN: 0-89448-120-7 ANS Order Number 700101

FOREWORD

The American Nuclear Society, through its Thermal Hydraulics Division, has joined the American Society of Mechanical Engineers and the American Institute of Chemical Engineers in the organization of the Annual Heat Transfer Conference.

Accordingly, this volume represents the first issue of a series of annual proceedings. It contains the papers presented in the sessions organized by the American Nuclear Society in the first of these joint endeavors with ASME and AIChE, the 1985 National Heat Transfer Conference held in Denver, Colorado. These sessions covered thermal-hydraulic instabilities in nuclear reactor systems, computational modeling of thermal-fluid systems, thermal-hydraulic mechanisms for severe reactor accidents, and thermal-hydraulic aspects of nuclear reactor transients. Papers contributed to joint sessions with ASME and AIChE on multiphase flow and heat transfer are published in a separate symposium volume.

The ANS Thermal Hydraulics Division is proud of the high quality of its first direct contribution to the National Heat Transfer Conference and would like to express its thanks to all the authors, the Session Organizers and the ANS Publication Department.

M. D. Carelli
Chairman, National/
International
Heat Transfer Conferences
Subcommittee

Y. Y. Hsu
1985 Division Chairman

S. Levy
1985 Program Chairman
1986 Division Chairman

T. Theofanous
1986 Program Chairman

CONTENTS

ANS PROCEEDINGS - 1985 NATIONAL HEAT TRANSFER CONFERENCE

INDEX OF TECHNICAL PAPERS BY SESSIONS

THERMAL-HYDRAULIC INSTABILITIES IN NUCLEAR REACTOR SYSTEMS

Monday, August 5, 1985
(Morning)

Session Chairman: Richard T. Lahey, Jr.
Session Co-Chairman: Virgil E. Schrock

COMPUTATIONAL MODELLING OF THERMAL-FLUID SYSTEMS-I

Monday, August 5, 1985
(Afternoon)

Session Chairman: Sanjoy Banerjee
Session Co-Chairman: S. Patankar

COMPUTATIONAL MODELLING OF THERMAL-FLUID SYSTEMS-II

Tuesday, August 6, 1985
(Morning)

Session Chairman: Sanjoy Banerjee
Session Co-Chairman: S. Patankar

THERMAL-HYDRAULIC MECHANISMS FOR SEVERE REACTOR ACCIDENTS-I

Tuesday, August 6, 1985
(Morning)

Session Chairman: T. G. Theofanous
Session Co-Chairman: Hans Fauske

THERMAL-HYDRAULIC MECHANISMS FOR SEVERE REACTOR ACCIDENTS-II

Tuesday, August 6, 1985
(Afternoon)

Session Chairman: T. G. Theofanous
Session Co-Chairman: Hans Fauske

THERMAL-HYDRAULIC ASPECTS OF NUCLEAR REACTOR TRANSIENTS-I

Wednesday, August 7, 1985
(Morning)

Session Chairman: Y. Y. Hsu
Session Co-Chairman: R. Duffey

THERMAL-HYDRAULIC ASPECTS OF NUCLEAR REACTOR TRANSIENTS-II

Wednesday, August 7, 1985
(Afternoon)

Session Chairman: Y. Y. Hsu
Session Co-Chairman: R. Duffey

THERMAL-HYDRAULIC INSTABILITIES IN NUCLEAR REACTOR SYSTEMS

Session Chairman:

Richard T. Lahey, Jr.

Session Co-Chairman:

Virgil E. Schrock

Monday AM

August 5, 1985

OSCILLIATORY BEHAVIOR IN A NATURAL CONVECTION SODIUM LOOP

O. A. ADEKUGBE, A. L. SCHOR and M. S. KAZIMI
Massachusetts Institute of Technology
Cambridge, Massachusetts 02139
(617) 253-5233

ABSTRACT

The natural convection in a sodium-cooled loop is investigated. An approximate analytical approach is developed and used to predict the stability characteristics of the flow in this loop. The analytical expression is verified against numerical results of a more complex simulation and found to adequately predict the stability limit, for the configuration considered.

INTRODUCTION

The inherent safety advantages of possible post-accident (and post-shutdown) natural convection cooling of nuclear reactors have sustained an active interest in natural convection loop flows in Nuclear Engineering. Yoram Zvirin[1] investigated natural circulation loop flows in pressurized water reactors, and S. Kaizerman, E. Wacholder and E. Elias[2] further investigated the stability and transient behavior of water in a vertical toroidal loop. Their results have shown general agreement with the results of the earlier work by Creveling and co-workers.[3] It has been suggested[4] that natural convection may represent a significant heat removal mechanism for the loss-of-pipe integrity (LOPI) and loss-of-shutdown heat-removal system (LSHRS) accidents of Liquid Metal-Cooled Fast Breeder Reactors (LMFBR). In this work we investigate single-phase natural convection loop flow for sodium. The loop geometry considered is designed to simulate the Fast Test Reactors (FTR).[4] The existence of constant temperature plena between a heated section in such geometry and the use of liquid-sodium characterizes the present work.

The ultimate modeling of a complex thermal-hydraulic system such as a nuclear reactor will provide a generalized dynamical treatment in which the effective flow inertia, capacitance and resistance of the system are represented. Loop components such as nozzles, pumps and valves can be represented as hydromechanical transducers and transformers.[5]

In this work, a treatment is given for a simple primary loop of an LMFBR (simplified by the absence of pumps, nozzles and valves) in a one-dimensional flow model. The effective loop inertia, capacitance and resistance are obtained by summing the hydraulic component of each term to the contributions from the heating at the source (core) and cooling at the plena.

The results will provide a description of the onset of motion as well as metastable equilibrium conditions. Numerical results and analytical predictions are compared with regard to instability damping.

THE STEADY-STATE LOOP MASS FLOW RATE

The single-phase steady-state flow in the loop is governed by the laws of conservation of mass, momentum and energy as presented below in one-dimensional representation

$$\frac{dG}{ds} = 0 \tag{1}$$

$$\frac{1}{\rho_o}\frac{d(G^2)}{ds} = \frac{dP}{ds} - \frac{f|G|G}{2D_e\rho_o} + \rho(s)\vec{g}\cdot\hat{e} \tag{2}$$

$$\frac{d}{ds}(hG) = \frac{P_H q''_{source}}{A} - \frac{P_H q''_{sink}}{A} \tag{3}$$

where

- G is the mass flux
- $\rho(s)$ is the density at any spatial location in the loop.
- ρ_o is an initial (reference density)
- A_H is heat transfer area (both at source and sink)
- P_H is the heated perimeter in the source (and cooled perimeter in the sink)

q'' is the heat flux

s is the spatial coordinate that runs round the loop, and

$\hat{e}$ is a unit vector in the direction s.

Friction and form losses have been neglected in comparison to the source and sink terms in the energy equation (Eq. (3)), and the Bousinesq approximation has been adopted in obtaining the momentum equation (Eq. (2)).

Equation (1) is substituted into Eq. (2) and Eq. (3) to recast the momentum and energy equations as follows:

$$\frac{dP}{ds} + \frac{f|G|G}{2\,D_e\rho_o} = \rho(s)\vec{g}\cdot\hat{e} \qquad (4)$$

$$G\,\frac{dh}{ds} = \frac{P_H q''_{source}}{A} - \frac{P_H q''_{sink}}{A} \qquad (5)$$

The momentum equation (Eq. (4)) is integrated round the loop, the close loop integral of the change in pressure drops off and we obtain:

$$\int_{loop} \frac{f|G|G}{2\,D_e\rho_o}\,ds = -\beta\rho_o \int_{loop} \vec{g}\cdot\hat{e}\;T(s)ds \qquad (6)$$

where the linear dependence of density on temperature for sodium has been applied; that is,

$$\rho(s) = \rho_o(1 - \beta(T(s) - T_o)) \qquad (7)$$

β is the coefficient of thermal expansion.

The usual form of the correlation for friction factor is used to evaluate the left hand side of Eq. (6).

$$f = a\left(\frac{GD_e}{\mu}\right)^{-b} = a\left(\frac{WD_e}{\mu A}\right)^{-b} \qquad (8)$$

where W is the mass flow rate, and A is the tube's cross sectional area.

$$\frac{aW^{(2-b)}\mu^b L}{2\,D_e^{(1+b)}A^{(2-b)}\rho_o} = -\beta\rho_o \int_{loop} \vec{g}\cdot\hat{e}\;T(s)ds \qquad (9)$$

where L is the total length of the loop flow path.

Rewriting Eq. (5) as appropriate for the loop (Fig. 1), and using the mass flow rate and temperature as the dependent variables, we obtain the energy equation as:

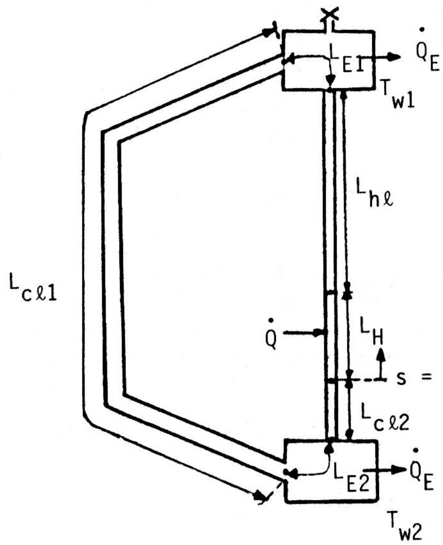

Fig. 1. **The loop modeling geometry.**

$$\frac{W}{A}\,C_p\,\frac{dT(s)}{ds} = \begin{cases} \dfrac{4q''}{D_e} & ;\ \text{heated section} \\ \dfrac{4h}{D_e}(T_{w1} - T(s)); & \text{upper plenum} \\ \dfrac{4h}{D_e}(T_{w2} - T(s)); & \text{lower plenum} \\ 0 & ;\ \text{cold \& hot legs} \end{cases} \qquad (10)$$

where h is the heat transfer coefficient between the liquid sodium and the plenum walls; for the purpose of integration, it will be assumed constant; actually, for liquid sodium, this is a rather mild assumption, especially at the low flows under consideration.

T_{w1} and T_{w2} are the constant temperatures of the upper and lower plenum respectively.

Equation (10) is integrated round the loop to obtain the steady state temperature distributions as:

$$T_1(s) = T_6 + \frac{\dot{Q}s}{C_p W L_H} ; \quad 0 \leq s \leq L_1$$

$$T_2(s) = T_6 + \frac{\dot{Q}}{WC_p} ; \quad L_1 \leq s \leq L_2$$

$$T_3(s) = T_{w1} + [\frac{\dot{Q}}{WC_p} - (T_{w1} - T_6)] \times \exp(\alpha(L_2 - s)); \; L_2 \leq s \leq L_3$$

$$T_4(s) = T_{w1} + [\frac{\dot{Q}}{WC_p} - (T_{w1} - T_6)] \times \exp(-\alpha L_{E1}); \quad L_3 \leq s \leq L_4$$

$$T_5(s) = T_{w2} + (T_{w1} - T_{w2}) \exp(\alpha(L_4 - s)) + (\frac{\dot{Q}}{WC_p} - (T_{w1} - T_6)) \times \exp(\alpha(L_3 - s)); \; L_4 \leq s \leq L_5,$$

and

$$T_6(s) = T_{w2} + (T_{w1} - T_{w2}) \exp(-\alpha L_{E1}) + (\frac{\dot{Q}}{WC_p} - T_{w1}) \exp(-\alpha(L_{E1} + L_{E2})); \quad L_5 \leq s \leq L \tag{11}$$

where

$$L_1 = L_H$$

$$L_2 = L_H + L_{h\ell}$$

$$L_3 = L_H + L_{h\ell} + L_{E1}$$

$$L_4 = L_H + L_{h\ell} + L_{E1} + L_{E\ell 1}$$

$$L_5 = L_H + L_{h\ell} + L_{E1} + L_{C\ell 1} + L_{E2}$$

$$L = L_H + L_{h\ell} + L_{E1} + L_{C\ell 1} + L_{E2} + L_{C\ell 2},$$

and

$$\alpha = \frac{4hA}{WC_p D_e} = \frac{4}{D_e} St \tag{12}$$

St = Stanton number

Using Eqs. (11) for the temperature to perform the integration in Eq. (9) we obtain an expression relating the steady state mass flow-rate to the input power, the loop geometry fluid properties and the regime of flow as:

$$\frac{aW^{(2-b)}\mu^b L}{2\beta g \rho_o^2 D_e^{(1+b)} A^{(2-b)}} + (T_{w1} - T_{w2})L_6 - \frac{\dot{Q}}{C_p W} L_7 - (T_{w1} - T_{w2})\{L_8 \exp(-\alpha L_{E1}) - L_9 \exp(-\alpha(L_{E1} + L_{E2}))\} - \frac{\dot{Q}}{WC_p}\{L_9 \exp(-\alpha(L_{E1} + L_{E2})) - L_{10} \exp(-\alpha L_{E1})\} = 0 \tag{13}$$

The additional geometrical parameters in Eq. (13) and (14) are defined as:

$$L_6 = L_H + L_{h\ell} + L_{C\ell 2} + L_{E2}/2$$

$$L_7 = L_H/2 + L_{h\ell} - 1/2\alpha$$

$$L_8 = 2L_H + 1/\alpha + 2L_{C\ell 2} + (L_{E1} + L_{E2})/2$$

$$L_9 = L_H + L_{C\ell 2} + 1/2\alpha$$

$$L_{10} = L_H + L_{h\ell} + L_{C\ell 2} + (L_{E1} + L_{E2})/2$$

For all practical loops, the heat transfer coefficient h is high and the equivalent diameter is reasonably small; the terms containing the exponentials in Eq. (13) can be neglected compared to the other terms. With little manipulation we have:

$$\frac{aW^{(3-b)}\mu^b C_p L}{\beta g \rho_o^2 D_e^{(2+b)} A^{(2-b)} \dot{Q}} + \frac{2WC_p}{\dot{Q} D_e}(T_{w2} - T_{w1}) L_6 - \frac{L_H + 2L_{h\ell}}{2D_e} + \frac{1}{4St} = 0 \tag{14a}$$

Numerical simulations of the ORNL loop[4] indicated a transition flow regime. The first term in Eq. (14a) is thus evaluated by a weighted sum of laminar and turbulent contributions:[7]

$$\left(\frac{aW^{(3-b)}\mu^b C_p L}{\beta g \rho_o^2 D_e^{(2+b)} A^{(2-b)} \dot{Q}}\right)_{lam}\sqrt{\psi}$$

$$+ \left(\frac{aW^{(3-b)}\mu^b C_p L}{\beta g \rho_o^2 D_e^{(2+b)} A^{(2-b)} \dot{Q}}\right)_{turb}\sqrt{1-\psi}$$

$$+ \frac{2WC_p}{\dot{Q}D_e}(T_{w2} - T_{w1})L_6 - \frac{L_H + 2L_{h\ell}}{2D_e} + \frac{1}{4St} = 0 \quad (14b)$$

where: $\psi = (Re - 400)/2200$,

$a = 64$, $b = 1$, for laminar flow

and $a = 0.316$, $b = .25$, for turbulent flow.

Equation (14b) has shown good agreement with experimental results and numerical calculations, for the ORNL experimental loop ORNL[2] as shown in Fig. 2.

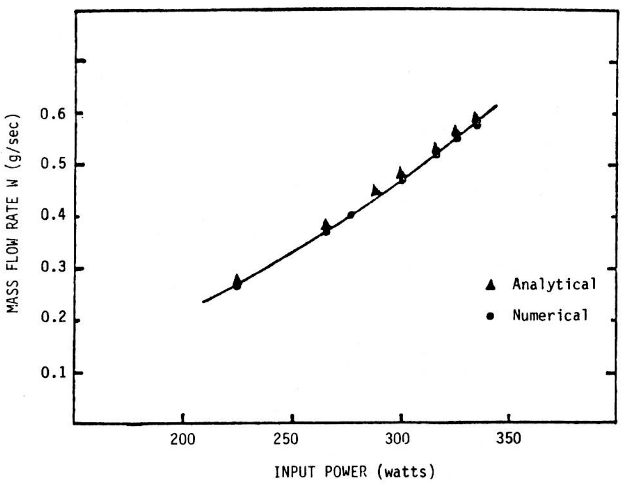

Fig. 2. Functional dependence of the mass flow rate on input power.

LOOP FLOW OSCILLATION ANALYSIS

The stability of flow in the loop is specified by considering the steady-state solution plus the space- and time-dependent perturbations of flow parameters, the approach closely following that of Creveling et al.[3] The following simplified time-dependent conservation equations are adequate for representing the transient state of flow in the loop:[6]

$$\frac{\partial}{\partial t}(\rho' + \bar{\rho}) + \frac{\partial}{\partial s}(\bar{G} + G') = 0 \quad (15)$$

$$\frac{\partial}{\partial t}(\bar{G} + G') + \frac{\partial}{\partial s}\left[\frac{(\bar{G} + G')^2}{\rho_o}\right] = - \frac{\partial}{\partial s}(\bar{p} + p') - f\frac{(\bar{G} + G')^2}{2 D_e \rho_o} - \frac{1}{C_T}\int^t G_T'(t')dt' + (\bar{\rho}+\rho')\vec{g}\cdot\hat{e} \quad (16)$$

$$\frac{\partial}{\partial t}[\rho_o(\bar{h} + h')] + \frac{\partial}{\partial s}[(\bar{h} + h')(\bar{G} + G')] = \frac{q''_{source}P_H}{A_H} - \frac{q''_{sink}P_H}{A_H} \quad (17)$$

In the above equations, we have assumed the following:

- The effect of the perturbation in the density is negligible in the acceleration and the frictional loss terms and in the enthalpy density (ρh).
- The steady-state correlations for friction factor f and the heat transfer coefficient implied in Eqs. (16) and (17), respectively, can be used. Welander[3] has pointed out that this is true whenever the advection time is large in comparison with the time for momentum or energy to diffuse across the tube's cross-section.

The primes are used to denote the perturbations in the various quantities while the bars are used to denote the steady-state values. G_T' and C_T are the perturbation in the mass flux into (or out of) the expansion tank, and the gravity tank capacitance respectively.[5]

$$C_T = \frac{A_T}{\rho_o g} \quad (18)$$

where A_T is the tank's flow cross-sectional area.

Subtracting the steady-state Eqs. (1), (2) and (3) from Eqs. (16), (17) and (18), and neglecting terms containing second and higher order of perturbations, we have the following equations for the perturbations of the mass flux and temperature:

$$L \frac{d}{dt} G'(t) = \frac{- a\mu^b (2-b)\, \overline{G}^{(1-b)} L}{2D_e^{(1+b)} \rho_o} G'(t)$$

$$- \frac{1}{C_T} \int^t G_T(t')dt'$$

$$- \rho_o \beta \int_{loop} \hat{e} \cdot \vec{g}\; T'(t,s)ds \quad (19)$$

$$\rho_o C_p \frac{\partial T'(t,s)}{\partial t} + \overline{G}\, C_p \frac{\partial T'(t,s)}{\partial s}$$

$$+ G'(t) C_p \frac{d\overline{T}(s)}{ds}$$

$$= \begin{cases} - \frac{4h}{D_e} T'(t,s); & \text{upper and lower plena} \\ 0 & ; \text{otherwise} \end{cases} \quad (20)$$

with the initial conditions

$$G'(0) = G'_o$$

$$T'(0,s) = 0 \quad (21)$$

We let

$$R' = - \frac{a\mu^b (2-b) \overline{G}^{(1-b)} L}{2D_e^{(1+b)} \rho_o} \quad (22a)$$

$$\frac{4h}{\rho_o C_p D_e} = \frac{\alpha W}{\rho_o A} \quad (22b)$$

where R' is the loop resistance corresponding to the flow of the perturbation in the mass flux G' and α is as defined in Eq. (12). Steady state heat injection at the source and extraction at the plena has been assumed, hence there are no perturbations in the heat fluxes; the dynamic state of flow is due to the initial perturbation in the mass flux.

Thus the assumption is made that thermal inertia of the heating system plays no role in this analysis, which is valid only for transients that are slow with respect to the time constant for conduction within the heaters.

The perturbation in the mass flux G' is assumed to be only time-dependent. This assumption can only be valid for single-phase flows in uniform cross-sectional tubes. The momentum equation has been integrated round the loop, hence the acceleration and the perturbation in pressure terms drop off, leading to the form of Eq. (20).

Next we define Laplace transforms as:

$$L[G'(t)] = \tilde{G}(z)$$

$$L[T'(t,s)] = \tilde{T}(z,s)$$

and take Laplace transforms of Eqs. (19) and (20) to have:

$$z\tilde{G}L - G'_o L = R'\tilde{G}$$

$$- \rho_o \beta \int_{loop} \hat{e} \cdot \vec{g}\; \tilde{T}\, ds + \frac{\tilde{G}_T}{C_T z} \quad (23)$$

$$z\tilde{T} + \frac{W}{A\rho_o} \frac{d\tilde{T}}{ds} + \frac{\tilde{G}}{\rho_o} \frac{d\overline{T}}{ds}$$

$$= \begin{cases} - \frac{\alpha W}{A\rho_o} \tilde{T} ; & \text{upper and lower plena} \\ 0 & ; \text{otherwise} \end{cases} \quad (24)$$

The perturbation in the buoyancy pressure drop ($\delta\tilde{P}_B$) driving the flow perturbation ($\tilde{G}$) round the loop is given by

$$\delta\tilde{P}_B = - \rho_o \int_{loop} \hat{e} \cdot \vec{g}\; \tilde{T} ds \quad (25)$$

The close loop integral in Eq. (25) simplifies for the loop in which the upper and lower plena are maintained at constant temperatures even during transients. Then the magnitude of T' is small in the return adiabatic leg compared to the heated section and the adjoining riser section. Thus we have:

$$\delta\tilde{\rho}_B = \rho_o \beta g \left\{ \int_o^{L_1} \tilde{T}_1\, ds + \int_{L_1}^{L_2} \tilde{T}_2\, ds \right\} \quad (26)$$

The temperature distribution $\tilde{T}_1$ and $\tilde{T}_2$ must be obtained and the integration indicated in Eq. (26) performed. The result obtained should be combined with Eq. (23) to obtain the perturbation in the mass flux as a function of the frequency domain variable z and of space.

Equation (24) is integrated round the loop and combined with the steady-state profiles of Eq. (17) to yield the required profiles of the perturbations in the temperature $\tilde{T}_1$ and $\tilde{T}_2$:[4,6]

$$\tilde{T}_1(z,s) = - \frac{\dot{Q}\tilde{G}}{\rho_o W C_p L_H z} + K_1 \exp\left(- \frac{A\rho_o z}{W} s\right);$$

$$0 \leq s \leq L_1 \quad (27a)$$

$$\tilde{T}_2(z,s) = K_2 \exp\left(-\frac{A\rho_o z}{W} s\right); \quad L_1 \le s \le L_2 \tag{27b}$$

where

$$K_1 = \frac{\dot{Q}\tilde{G}}{\rho_o C_p W L_H z} \exp\left(-\frac{A\rho_o L_H}{2W} z\right)$$
$$- \frac{\alpha \tilde{G}}{\rho_o z} (T_{w1} - T_{w2}) \exp(-\alpha L_E)$$
$$\times \exp\left(-\frac{A\rho_o L_E}{2W} z\right) + \frac{\alpha \tilde{G}}{\rho_o z} (T_{w1} - T_{w2})$$
$$\times \exp(-\alpha L_E) \exp\left(\frac{A\rho_o L_E}{2W} z\right)$$
$$+ \frac{\alpha \tilde{G}}{\rho_o z} \left(T_{w1} - T_{w2} + \frac{\dot{Q}}{WC_p}\right)$$
$$\times \exp\left(-\frac{3\alpha L_E}{2}\right) \exp\left(-\frac{A\rho_o L_E}{2W} z\right)$$
$$- \frac{\alpha \tilde{G}}{\rho_o z} \exp(-2\alpha L_E) \exp\left(\frac{A\rho_o L_H}{2W} z\right)$$
$$- \frac{\alpha \tilde{G}}{\rho_o z} \left(T_{w1} - T_{w2} + \frac{\dot{Q}}{WC_p}\right)$$
$$\times \exp(-2\alpha L_E) \exp\left(-\frac{A\rho_o L_E}{2W} z\right) \tag{28}$$

Considering orders of magnitude, the fourth and sixth terms can be neglected compared to the second and third terms, and the fifth term is negligible compared to the first term. This is satisfactory for $\alpha L_E << 1$, a condition that is always satisfied for all practical values of heat transfer coefficient and loop dimensions. Then,

$$K_1 = \frac{\dot{Q}\tilde{G}}{\rho_o C_p W L_H z} \exp\left(-\frac{A\rho_o L_H}{2W} z\right)$$
$$+ \frac{2\alpha \tilde{G}}{\rho_o z} (T_{w1} - T_{w2}) \exp(-\alpha L_E)$$
$$\times \sinh\left(\frac{A\rho_o L_E}{2W} z\right) \tag{29}$$

$$K_2 = -\frac{\dot{Q}\tilde{G}}{WC_p \rho_o L_H z} \exp\left(\frac{A\rho_o L_H}{2W} z\right) + K_1 \tag{30}$$

Using these expressions in Eq. (27) and performing the integration indicated in Eq. (26), we obtain the following expression for $\delta\tilde{P}_B$.

$$\delta\tilde{P}_B = \tilde{G}\rho_o \beta g \Big\{ -\frac{\dot{Q}}{\rho_o C_p W z} + \frac{2\dot{Q}}{A\rho_o^2 C_p L_H z^2}$$
$$\times \exp\left(-\frac{A\rho_o L_H}{2W} z\right) \sinh\left(\frac{A\rho_o L_H}{2W} z\right)$$
$$+ \frac{4W\alpha}{A\rho_o^2 z^2} (T_{w1} - T_{w2}) \exp(-\alpha L_E)$$
$$\times \sinh\left(\frac{A\rho_o L_E}{2W} z\right) \sinh\left(\frac{A\rho_o L_H}{2W} z\right)$$
$$+ \frac{\dot{Q}}{A\rho_o^2 C_p L_H z^2} \left(\exp\left(-\frac{A\rho_o L_{h\ell}}{W} z\right) - 1\right)$$
$$- \frac{2\alpha W}{A\rho_o^2 z^2} (T_{w1} - T_{w2}) \exp(-\alpha L_E)$$
$$\times \exp\left(-\frac{A\rho_o L_E}{2W} z\right)$$
$$\times \left(\exp\left(-\frac{A\rho_o L_{h\ell}}{W} z\right) - 1\right)$$
$$\times \sinh\left(\frac{A\rho_o L_E}{2W} z\right)\Big\} \tag{31}$$

Equation (23) becomes

$$\tilde{G}\Big\{ zL - R' - \rho_o \beta g \Big[-\frac{\dot{Q}}{\rho_o C_p W z} + \frac{2\dot{Q}}{A\rho_o^2 C_p L_H z^2}$$
$$\times \exp\left(-\frac{A\rho_o L_H}{2W} z\right) \sinh\left(\frac{A\rho_o L_H}{2W} z\right)$$
$$+ \frac{4\alpha W}{A\rho_o^2 z^2} (T_{w1} - T_{w2}) \exp(-\alpha L_E)$$
$$\times \sinh\left(\frac{A\rho_o L_E}{2W} z\right) \sinh\left(\frac{A\rho_o L_H}{2W} z\right)$$
$$+ \frac{\dot{Q}}{A\rho_o^2 C_p L_H z^2} \left(\exp\left(-\frac{A\rho_o L_{h\ell}}{W} z\right) - 1\right)$$
$$- \frac{2\alpha W}{A\rho_o^2 z^2} (T_{w1} - T_{w2}) \exp(-\alpha L_E)$$
$$\times \exp\left(-\frac{A\rho_o L_E}{2W} z\right)\left(\exp\left(-\frac{A\rho_o L_{h\ell}}{W} z\right) - 1\right)$$

$$x \sinh\left(\frac{A\rho_o L_E}{2W} z\right)\Big]\Big\} = G_o' L \qquad (32)$$

The gravity-tank capacitance term has been neglected with the assumption of a large tank.

Equation (32) can be written as

$$\tilde{G}(z)\, Y(z) = G_o'\, L \qquad (33)$$

From Eq. (33) we obtain the transfer function as:

$$H(z) = \frac{G_o'\, L}{Y(z)} \qquad (34)$$

H(z) is highly transcendental and rigorous stability characteristics can be obtained by employing Nyquist analysis.[3]

Single phase flow oscillation frequencies in the range of 0.005 Hz to 0.025 Hz have been obtained experimentally and numerically for liquid water loops,.[2,3,8] Creveling[3] has also pointed out that low frequencies are anticipated for single-phase liquid oscillations in general.

In view of the anticipated low frequencies, a second order approximation has been deemed sufficient to represent the dynamic state of flow in the loop.

The exponential and hyperbolic functions in Eq. (34) are expanded in Taylor series about z = 0 such that the resulting expression is second order in z.[6] We obtain:

$$\tilde{G}\left[ez^2 + fz + c\right] = zG_o'\, L \qquad (35)$$

where e, f and c are defined by:

$$e = L - \frac{\dot{Q}\beta g\rho_o^2 A^2 L_H^2}{6W^3 C_p} - \frac{A^2\rho_o^2\beta g}{24W^2}$$

$$x\ (T_{w1} - T_{w2})\alpha\ L_E \exp(-\ \alpha\ L_E) \qquad (36a)$$

$$f = \frac{\dot{Q}\beta g\rho_o A L_H}{24W^2 C_p} - R' - \frac{\beta g\rho_o A}{2W}\ (T_{w1} - T_{w2})$$

$$x\ L_H\alpha\ L_E \exp(-\ \alpha\ L_E) \qquad (36b)$$

$$c = \frac{\beta g\dot{Q}}{WC_p} - \rho g(T_{w1} - T_{w2})\alpha\ L_E \exp(-\alpha\ L_E) \qquad (36c)$$

From Eq. (35) we obtain:

$$\tilde{G} = \frac{z\ L/e\ G_o'}{(z+\sigma)^2 + \omega^2} \qquad (37)$$

where

$$\sigma = f/2e \qquad (38a)$$

$$\omega^2 = c/e - \sigma^2 \qquad (38b)$$

Obtaining the inverse Laplace transform of Eq. (37), we have the response function as:

$$G'(t) = A \exp(-\sigma t) \sin(\omega t + \phi) \qquad (39)$$

where

$$\phi = \tan^{-1}(\omega/\sigma)$$

$$A = \frac{G_o'\ L}{e} \operatorname{cosec}\phi$$

STABILITY CRITERION

For stability, the damping factor σ must be greater than zero, marginal stability being provided by equality. Hence

$$\sigma = f/23 \geq 0$$

With W in Eq. (36) prescribed greater than the anticipated steady-state value corresponding to the input power, $e > 0$.[6] Thus, for stability we must have:

$$f \geq 0$$

Or from the definition of f in Eq. (36)

$$-\frac{R'W^2}{\beta g\rho_o A} - \frac{W}{2}(T_{w1} - T_{w2})L_H\ \alpha\ L_E$$

$$x \exp(-\ \alpha\ L_E) + \frac{\dot{Q}L_H}{24C_p} \geq 0 \qquad (40)$$

It should be noted that the W that appears in Eq. (40) is the initial mass flow rate which includes the initial flow perturbation.

NUMERICAL EXAMPLE

Instability was not reported for single-phase in the Oak Ridge experiment.[4] Our analytical expressions also predict that liquid single-phase flow in this particular loop is stable for all input powers. However, other researchers have reported experimentally observed oscillatory behavior and instabilities in single-phase loop systems.[2,3,8]

Moreover, it has been pointed out that flow stability depends strongly on the loop frictional resistance[3] as well as loop geometry.

In order to test our analytical approach and gain insight into the phenomenon, we have used the loop version of the thermal-hydraulic code-THERMIT-4E[6,7] to simulate flow oscillations in the loop. Oscillation and instability were induced by artificially reducing the loop resistance, thereby reducing its intrinsic damping characteristics.

Specifically for the purpose of obtaining oscillation the friction factor was correlated as:

$$f = 0.1099 \; Re^{-0.25} \qquad (41)$$

f as calculated in Eq. (41) reduces the loop resistance by a factor of about ten compared to the values obtained from the actual correlation used in Eq. (14b).

The results of the calculations in Table 1 show that flow is unstable at $\dot{Q}$ = 150 Watts. At higher power levels Eq. (38a) predicts that flow is stable, with increasing damping factors. At lower powers than 150 Watts Eq. (38a) predicts that the flow remains unstable. It should be pointed out that near zero power, the system may become stable again, as has been observed experimentally for a toroidal loop.[2] We have not investigated that power range. A general trend of increasing damping with increasing input power is predicted analytically as illustrated in Fig. 3. The flow responses obtained from the code's results illustrated in Fig. 4, also depict increasing damping with increasing power. Flow actually reverses at 150 Watts.

Table 1 also shows the values of frequencies (F) predicted by Eq. (38b) and the values obtained from the numerical simulations. Frequencies of 0.020 Hz and 0.021 Hz are predicted for input powers of 150 Watts and 250 Watts respectively. These values agree within 20% with the code's predictions of 0.022 Hz and 0.023 Hz respectively. These values also fall within the range of 0.005 Hz to 0.025 Hz that has been obtained experimentally and numerically for low pressure single-phase water loops.[2,3,8]

6. CONCLUSION

A simplified analytical expression derived for the marginal stability limit of a flow loop is verified by numerical results of more exact equations. It would be somewhat more demanding but still straightforward to apply this analytical approach to reactor plant conditions.

REFERENCES

1. Yoram Zvirin, "A Review of Natural Circulation Loops in Pressurized Water Reactors and other Systems," Nuclear Eng. and Design 67 (1981) 203-225.

2. S. Kaizerman, E. Wacholder and E. Elias, "Stability and Transient Behavior of a Vertical Toroidal Thermosyphon," ASME Winter Annual Meeting, Nov. 15-20, 1981.

3. H. F. Creveling, J. F. De Paz, J. Y. Baladi and R. J. Schonhals, "Stability Characteristics of Single-Phase Free Convection Loop," J. Fluid Mech. (1975), vol. 67, Part 1, pp. 65-84.

4. P. W. Garrison, R. H. Morris and B. H. Montgomery, "Dryout Measurements for Sodium Natural Convection in a Vertical Channel," Oak Ridge National Laboratory Report; ORNL, TM-7018, Dec. 1979.

5. R. C. Rosenberg and D. C. Karnopp, Introduction to Physical Systems Dynamics, McGraw-Hill (1983).

6. O. A. Adekugbe, A. L. Schor and M. S. Kazimi, "Loop Simulation Capability for Sodium-Cooled Systems," MIT Energy Laboratory Report; MIT-EL 84-013, June 1984.

7. A. L. Schor and N. E. Todreas, "A Four-Equation Two-Phase Flow Model for Sodium Boiling Simulation of LMFBR Fuel Assemblies," MIT Energy Laboratory Report No. MIT-EL 82-039, December 1982.

8. E. Wacholder, S. Kaizerman and E. Elias, "A Numerical Analysis of the Stability and Transient Behavior of Natural Convection Loops," Letters In Applied and Engineering Sciences, IJESAN 20(11) 1181-1274 (1982).